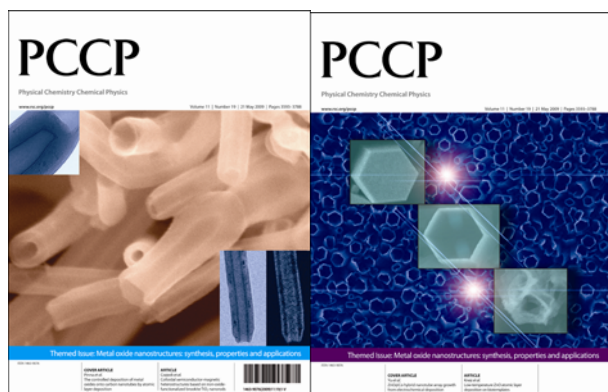


This paper is published as part of a PCCP Themed Issue on:  
[Metal oxide nanostructures: synthesis, properties and applications](#)



Guest Editors: Nicola Pinna, Markus Niederberger, John Martin Gregg and Jean-Francois Hochepeid

## Editorial

### [Chemistry and physics of metal oxide nanostructures](#)

*Phys. Chem. Chem. Phys.*, 2009

DOI: [10.1039/b905768d](#)

## Papers

### [Thermally stable ordered mesoporous CeO<sub>2</sub>/TiO<sub>2</sub> visible-light photocatalysts](#)

Guisheng Li, Dieqing Zhang and Jimmy C. Yu, *Phys. Chem. Chem. Phys.*, 2009

DOI: [10.1039/b819167k](#)

### [Blue nano titania made in diffusion flames](#)

Alexandra Teleki and Sotiris E. Pratsinis, *Phys. Chem. Chem. Phys.*, 2009

DOI: [10.1039/b821590a](#)

### [Shape control of iron oxide nanoparticles](#)

Alexey Shavel and Luis M. Liz-Marzán, *Phys. Chem. Chem. Phys.*, 2009

DOI: [10.1039/b822733k](#)

### [Colloidal semiconductor/magnetic heterostructures based on iron-oxide-functionalized brookite TiO<sub>2</sub> nanorods](#)

Raffaella Buonsanti, Etienne Snoeck, Cinzia Giannini, Fabia Gozzo, Mar Garcia-Hernandez, Miguel Angel Garcia, Roberto Cingolani and Pantaleo Davide Cozzoli, *Phys. Chem. Chem. Phys.*, 2009

DOI: [10.1039/b821964h](#)

### [Low-temperature ZnO atomic layer deposition on biotemplates: flexible photocatalytic ZnO structures from eggshell membranes](#)

Seung-Mo Lee, Gregor Grass, Gyeong-Man Kim, Christian Dresbach, Lianbing Zhang, Ulrich Gösele and Mato Knez, *Phys. Chem. Chem. Phys.*, 2009

DOI: [10.1039/b820436e](#)

### [A LEEM/LEED investigation of phase transformations in TiO<sub>2</sub>/Pt\(111\) ultrathin films](#)

Stefano Agnoli, T. Onur Menteş, Miguel A. Niño, Andrea Locatelli and Gaetano Granozzi, *Phys. Chem. Chem. Phys.*, 2009

DOI: [10.1039/b821339a](#)

### [Synthesis and characterization of V<sub>2</sub>O<sub>5</sub> nanorods](#)

Alexander C. Santulli, Wenqian Xu, John B. Parise, Liusuo Wu, M.C. Aronson, Fen Zhang, Chang-Yong Nam, Charles T. Black, Amanda L. Tiano and Stanislaus S. Wong, *Phys. Chem. Chem. Phys.*, 2009

DOI: [10.1039/b822902c](#)

### [Flame spray-pyrolyzed vanadium oxide nanoparticles for lithium battery cathodes](#)

See-How Ng, Timothy J. Patey, Robert Büchel, Frank Krumeich, Jia-Zhao Wang, Hua-Kun Liu, Sotiris E. Pratsinis and Petr Novák, *Phys. Chem. Chem. Phys.*, 2009

DOI: [10.1039/b821389p](#)

### [Mesoporous sandwiches: towards mesoporous multilayer films of crystalline metal oxides](#)

Rainer Ostermann, Sébastien Sallard and Bernd M. Smarsly, *Phys. Chem. Chem. Phys.*, 2009

DOI: [10.1039/b820651c](#)

### [Surprisingly high, bulk liquid-like mobility of silica-confined ionic liquids](#)

Ronald Göbel, Peter Hesemann, Jens Weber, Eléonore Möller, Alwin Friedrich, Sabine Beuermann and Andreas Taubert, *Phys. Chem. Chem. Phys.*, 2009

DOI: [10.1039/b821833a](#)

### [Fabrication of highly ordered, macroporous Na<sub>2</sub>W<sub>2</sub>O<sub>7</sub> arrays by spray pyrolysis using polystyrene colloidal crystals as templates](#)

SunHyung Lee, Katsuya Teshima, Maki Fujisawa, Syuji Fujii, Morinobu Endo and Shuji Oishi, *Phys. Chem. Chem. Phys.*, 2009

DOI: [10.1039/b821209k](#)

### [Nanoporous Ni-Ce<sub>0.8</sub>Gd<sub>0.2</sub>O<sub>1.9-x</sub> thin film cermet SOFC anodes prepared by pulsed laser deposition](#)

Anna Infortuna, Ashley S. Harvey, Ulrich P. Muecke and Ludwig J. Gauckler, *Phys. Chem. Chem. Phys.*, 2009

DOI: [10.1039/b821473e](#)

### [Surface chemistry of carbon-templated mesoporous aluminas](#)

Thomas Onfroy, Wen-Cui Li, Ferdi Schüth and Helmut Knözinger, *Phys. Chem. Chem. Phys.*, 2009

DOI: [10.1039/b821505g](#)

### [ZnO@Co hybrid nanotube arrays growth from electrochemical deposition: structural, optical, photocatalytic and magnetic properties](#)

Li-Yuan Fan and Shu-Hong Yu, *Phys. Chem. Chem. Phys.*, 2009

DOI: [10.1039/b823379a](#)

### [Electrochemistry of LiMn<sub>2</sub>O<sub>4</sub> nanoparticles made by flame spray pyrolysis](#)

T. J. Patey, R. Büchel, M. Nakayama and P. Novák, *Phys. Chem. Chem. Phys.*, 2009

DOI: [10.1039/b821572n](#)

### [Ligand dynamics on the surface of zirconium oxo clusters](#)

Philip Walther, Michael Puchberger, F. Rene Kogler, Karlheinz Schwarz and Ulrich Schubert, *Phys. Chem. Chem. Phys.*, 2009

DOI: [10.1039/b820731c](#)

**[Thin-walled Er<sup>3+</sup>:Y<sub>2</sub>O<sub>3</sub> nanotubes showing up-converted fluorescence](#)**

Christoph Erk, Sofia Martin Caba, Holger Lange, Stefan Werner, Christian Thomsen, Martin Steinhart, Andreas Berger and Sabine Schlecht, *Phys. Chem. Chem. Phys.*, 2009

DOI: [10.1039/b821304f](#)

**[Wettability conversion of colloidal TiO<sub>2</sub> nanocrystal thin films with UV-switchable hydrophilicity](#)**

Gianvito Caputo, Roberto Cingolani, Pantaleo Davide Cozzoli and Athanassia Athanassiou, *Phys. Chem. Chem. Phys.*, 2009

DOI: [10.1039/b823331d](#)

**[Nucleation and growth of atomic layer deposition of HfO<sub>2</sub> gate dielectric layers on silicon oxide: a multiscale modelling investigation](#)**

A. Dkhissi, G. Mazaleyrat, A. Estève and M. Djafari Rouhani, *Phys. Chem. Chem. Phys.*, 2009

DOI: [10.1039/b821502b](#)

**[Designing meso- and macropore architectures in hybrid organic-inorganic membranes by combining surfactant and breath figure templating \(BFT\)](#)**

Ozlem Sel, Christel Laberty-Robert, Thierry Azais and Clément

Sanchez, *Phys. Chem. Chem. Phys.*, 2009

DOI: [10.1039/b821506e](#)

**[The controlled deposition of metal oxides onto carbon nanotubes by atomic layer deposition: examples and a case study on the application of V<sub>2</sub>O<sub>5</sub> coated nanotubes in gas sensing](#)**

Marc-Georg Willinger, Giovanni Neri, Anna Bonavita, Giuseppe Micali, Erwan Rauwel, Tobias Hertrich and Nicola Pinna, *Phys. Chem. Chem. Phys.*, 2009

DOI: [10.1039/b821555c](#)

**[In situ investigation of molecular kinetics and particle formation of water-dispersible titania nanocrystals](#)**

G. Garnweitner and C. Grote, *Phys. Chem. Chem. Phys.*, 2009

DOI: [10.1039/b821973g](#)

**[Chemoresistive sensing of light alkanes with SnO<sub>2</sub> nanocrystals: a DFT-based insight](#)**

Mauro Epifani, J. Daniel Prades, Elisabetta Comini, Albert Cirera, Pietro Siciliano, Guido Faglia and Joan R. Morante, *Phys. Chem. Chem. Phys.*, 2009

DOI: [10.1039/b820665a](#)

# Wettability conversion of colloidal TiO<sub>2</sub> nanocrystal thin films with UV-switchable hydrophilicity

Gianvito Caputo,<sup>ab</sup> Roberto Cingolani,<sup>ac</sup> Pantaleo Davide Cozzoli<sup>\*ab</sup> and Athanassia Athanassiou<sup>\*ac</sup>

Received 6th January 2009, Accepted 5th March 2009

First published as an Advance Article on the web 26th March 2009

DOI: 10.1039/b823331d

Under pulsed laser UV irradiation, thin-film coatings made of close-packed TiO<sub>2</sub> nanorods individually coated with surfactants can exhibit a temporary increase in their degree of surface hydroxylation without any apparent photocatalytic removal of the capping molecules. This mechanism provides a basis for achieving light-driven conversion from a highly hydrophobic to a highly hydrophilic, metastable state, followed by extremely slow recovery of the original conditions under dark ambient environment. A deeper insight into the wetting dynamics is gained by time-dependent water contact-angle and infrared spectroscopy monitoring of the film properties under different post-UV storage conditions. Our study reveals that, for reversible switchability between extreme wettability excursions and long-term repeatability of such changes to be achieved, specific modifications in the polar and nonpolar components of the TiO<sub>2</sub> films need to be guaranteed along with preservation of the original geometric arrangement of the nanocrystal building blocks. The application of moderate vacuum is found to be an effective method for accelerating the post-UV hydrophilic-to-hydrophobic conversion, thereby enabling fast and cyclic hydrophilization/hydrophobicization alternation without any detrimental signs of significant fatigue.

## 1. Introduction

The ability to engineer surfaces with dynamically modifiable wetting properties represents an actively pursued research area in materials science due to its implications in disparate technological fields, including sensing, microelectronics, cell manipulation, food technology, microfluidics, and design of smart multifunctional coatings and membranes.<sup>1–6</sup> There are two widely exploited classes of strategies for realizing surfaces that can display tailored and switchable wettability upon application of external stimuli. One approach involves surface functionalization with selected organic molecules that exhibit reversible changes in their dipole moment following structural transitions induced by either light irradiation, electric fields, pH or solvent changes.<sup>7–11</sup> The typical degree interval over which excursions in water contact angle (WCA) are achievable by these methods is, however, limited to about  $\sim 10$ – $15^\circ$  only, which can be only slightly extended by enhancing the roughness of the solid surface underneath.<sup>1–4,6–11</sup> An alternative and more powerful strategy relies on the capability of some transition-metal oxides, namely ZnO,<sup>12</sup> WO<sub>3</sub>,<sup>13</sup> V<sub>2</sub>O<sub>5</sub><sup>14</sup> and TiO<sub>2</sub>,<sup>3,15–18</sup> to increase their hydrophilicity under band-gap photoexcitation, and to revert back to the initial condition

upon storage in the dark. Besides offering long-term reproducible performances due to their inherent chemical resistance, such oxide materials can exhibit WCA variations as large as  $\sim 30$ – $70^\circ$  already in the form of smooth substrates, which can be ultimately amplified up to the  $180^\circ$  limit (*i.e.*, corresponding to superhydrophobic-to-superhydrophilic transitions) upon controlled introduction of extra micro- and nano-scale surface structuring.<sup>1–6,9–17</sup>

Among the aforementioned materials, TiO<sub>2</sub> represents an exclusive platform on which UV-light-stimulated wettability changes are triggered concertedly with the semiconductor photocatalytic activity. Joint exploitation of these two processes has indeed enabled development of unique multifunctional coatings simultaneously exhibiting self-cleaning, antibacterial, and antifogging properties.<sup>5,15,16</sup> Despite such technological potential, the understanding of the reversible photoswitchable wettability of TiO<sub>2</sub> remains a subject of intense debate. In one mechanistic picture, TiO<sub>2</sub> hydrophilicization has been rationalized as arising from sequential surface photocorrosion and reconstruction processes, which would involve hole-driven creation of surface oxygen vacancy defects on one side, and their healing upon molecular and/or dissociative adsorption of atmospheric water, on the other side.<sup>3,15–17,19–21</sup> Slow recovery of the starting surface condition then occurs under ambient storage in the dark due to atmospheric oxygen replacing the newly implanted hydroxyl moieties. Alternatively, it has been proposed that UV-driven hydrophylicization results from photocatalytic removal of adsorbed hydrophobic alkyl compounds (*e.g.* hydrocarbons), following which a new contaminating organic layer is

<sup>a</sup> National Nanotechnology Laboratory of CNR-INFM, Unità di Ricerca IIT, Distretto Tecnologico ISUFI, via per Arnesano km 5, 73100, Lecce, Italy. E-mail: athanassia.athanassiou@unile.it, davide.cozzoli@unile.it

<sup>b</sup> Scuola Superiore ISUFI, University of Salento, Distretto Tecnologico, Via per Arnesano km 5, 73100, Lecce, Italy

<sup>c</sup> IIT-Italian Institute of Technology, Via Morego 30, 16152, Genova, Italy

deposited upon prolonged dark storage.<sup>22–26</sup> However, discrepancies among main mechanistic conclusions should not necessarily be considered contradictory or mutually exclusive, owing to the broad variety of TiO<sub>2</sub> surfaces that have been probed by vastly different techniques under diverse measurement conditions.

In order to boost the technological potential of the reversibly photoinduced TiO<sub>2</sub> wettability, research activities have been intensively devoted to enhance the rate and the ultimate degree of hydrophilic conversion of TiO<sub>2</sub>-based substrates by carefully engineering surface roughness,<sup>3,15–18,27</sup> applying anodic polarization,<sup>28</sup> doping,<sup>29</sup> and/or creating composite heterostructures whereby TiO<sub>2</sub> sections are intimately connected to other semiconductor domains with suitably staggered band gaps (*e.g.* WO<sub>3</sub>).<sup>29–31</sup> On the other hand, although it would be highly desirable to devise strategies for affecting post-irradiation recovery of the pristine hydrophobicity status, earlier attempts have been limited to the use of either thermal or ultrasound treatments,<sup>21,32–34</sup> oxygenation<sup>21</sup> and visible irradiation,<sup>35</sup> albeit the relevant mechanistic implications have not yet been conclusive. The ability of reverting the wettability conditions of TiO<sub>2</sub> surfaces in a deliberate and fast way remains one of the most important goals that need to be achieved for enabling practical exploitation of such materials, for example, in microfluidics.

So far, the UV-switchable wettability of TiO<sub>2</sub> has been studied on micro-/nano-structured films grown directly onto substrates *via* sputtering, chemical vapour deposition, or sol-gel reaction/calcination, which are economically restrictive for large-scale applications. As a valuable alternative route, the assembly of preformed wet-chemically synthesized organic-free nanocrystals on substrates has been proposed for the fabrication of nanoporous coatings with superhydrophilic properties that, however, do not necessarily require UV irradiation to maintain their stability.<sup>31,36,37</sup>

More recently, we have demonstrated for the first time the feasibility of exploiting anatase TiO<sub>2</sub> nanorods (NRs) provided with an organic surfactant capping for the creation of close-packed thin-film coatings on a variety of inorganic and polymeric substrates with pre-engineered micro-roughness, which showed a reversible transition from a highly hydrophobic to a very hydrophilic state (with excursions in WCA values larger than  $\sim 100^\circ$ ) upon 355 nm pulsed laser photoexcitation.<sup>38–40</sup> The intense and intermittent irradiation regime triggers a peculiar hydrophilicization mechanism, according to which the degree of surface hydroxylation increases selectively at the organic-free domains of the TiO<sub>2</sub> NR facets, while the pre-existing anchored surfactants are not subjected to any noticeable photocatalytic degradation. Prolonged sample storage in the dark under ambient conditions allows the initial hydrophobicity to be fully restored.<sup>38–40</sup> The convenience of using such NRs for building UV-responsive oxide films stands within their peculiar structure and shape anisotropy. Actually, the preferential NR elongation along the *c*-axis direction of the anatase lattice can favour delocalization of photoexcited charge carriers, and hence their efficient utilization in the creation of surface vacancies. Additionally, the dominant (011)/(101)-type facets at the

NR surface are known to be particularly effective in the light-induced hydrophilicization mechanism of TiO<sub>2</sub>.<sup>38,41</sup>

In this contribution we investigate the kinetics of the post-irradiation dehydrophilicization of such type of colloidal TiO<sub>2</sub> NR based coatings following application of different external stimuli. Surfactant-coated TiO<sub>2</sub> thin films can be conveniently regarded as model platforms to study the mechanism of hydrophobicity recuperation of UV-treated organic-capped nanocrystals, since any impact on the organic (*i.e.*, related to the surfactant coating) and/or inorganic components (*i.e.*, associated with TiO<sub>2</sub> lattice and surface chemistry) in such systems can be clearly recognized and discriminated, as previously demonstrated for the forward hydrophilicization process.<sup>38–40</sup> In particular, the effects of applying either vacuum, combined visible/infrared laser illumination, and substrate heating on the ultimate wettability changes of the films have been examined by time-dependent WCA and Fourier transform infrared spectroscopy (FT-IR) measurements, and comparatively discussed with respect to their otherwise natural evolution under ambient dark condition taken as the reference. Our study reveals that, for reversible switchability between extreme wetting conditions and long-term repeatability of such changes to be guaranteed, dynamic changes in the polar and nonpolar components of the TiO<sub>2</sub> films need also to be guaranteed along with preservation of the original geometric arrangement of the nanocrystal building blocks. In contrast to previous findings,<sup>21,32–35</sup> we have observed that the application of moderate vacuum conditions is the most effective method for remarkably accelerating the post-UV hydrophilic-to-hydrophobic conversion, thereby enabling cyclic hydrophilicization/hydrophobicization alternation without any significant fatigue.

## 2. Experimental

### Materials

All chemicals were of the highest purity available and were used as received. Titanium tetraisopropoxide (Ti(OPr<sup>*i*</sup>)<sub>4</sub> or TTIP, 97%), trimethylamine *N*-oxide dihydrate ((CH<sub>3</sub>)<sub>3</sub>NO·2H<sub>2</sub>O or TMAO, 98%), oleic acid (C<sub>17</sub>H<sub>33</sub>CO<sub>2</sub>H or OLAC, 90%) were purchased from Aldrich. All solvents used were of analytical grade and were also purchased from Aldrich. Water was bidistilled (Millipore Q). Silicon (100) p-type slabs were purchased from Jocom.

### Synthesis of TiO<sub>2</sub> nanorods (NRs)

The synthesis carried out using a standard Schlenk line setup. Organic-capped anatase TiO<sub>2</sub> NRs with an average diameter of 3–4 nm and a mean length of 25–30 nm were obtained by TMAO-catalyzed hydrolysis of TTIP in OLAC acting as both solvent and stabilizing ligand.<sup>41</sup> In a typical synthesis, 15 mmol of TTIP dissolved in 70 g of degassed OLAC was reacted with 4 mL of an aqueous 2 M TMAO solution at 100 °C for 70 h under ambient atmosphere in a close vessel. The NRs were separated from their growing mixture upon 2-propanol addition and were subsequently subjected to repeated purification cycles of re-dispersion in toluene and precipitation with 2-propanol to wash out unreacted precursor



and excess surfactant molecules. At this point, the NRs were provided with a fresh OLAC capping layer by a ligand-exchange procedure, which involved stirring the NRs for 12 h at 80 °C in OLAC under N<sub>2</sub> atmosphere. Finally, the NRs were extracted and purified, as described above. An optically clear TiO<sub>2</sub> stock dispersion in toluene was prepared, whose concentration was determined by inductively coupled plasma atomic emission (ICP-AES) measurements performed with a Varian Vista AX spectrometer.

#### Fabrication of TiO<sub>2</sub> NR based thin film coatings

Before use, the Si substrates (1 cm<sup>2</sup>) were immersed into 2-propanol for 10 min, then repeatedly rinsed with acetone, and, finally, dried with a nitrogen flow. A 500-μL volume of a 0.1 M TiO<sub>2</sub> NR stock dispersion was uniformly spread onto the surface of liquid water that half-filled a 250-mL beaker. After the organic solvent was evaporated, a slightly opaque floating TiO<sub>2</sub> film could be recognized on the water surface. At this point, the substrate was gently dipped into the solution and subsequently withdrawn at a rate of ~1 cm min<sup>-1</sup>. This sequence was repeated a few times (up to five), as needed. Finally, the TiO<sub>2</sub>-covered substrates were dried with a gentle nitrogen flow and kept under vacuum for 3 h prior to further use in the irradiation/storage experiments (see below). The thickness of the coating films was typically less than 0.5 μm, as measured by a profilometer (Alpha-Step 500, Tencor Instruments).

#### Characterization of the films

The size-morphological characterization of as-prepared NRs were routinely checked by low-resolution transmission electron microscopy (TEM) analysis performed with a Jeol Jem 1011 microscope operating at an accelerating voltage of 100 kV. The TiO<sub>2</sub> NR coatings deposited onto silicon substrates were imaged by scanning transmission microscopy (SEM) inspection carried out with FEI Nova NanoSEM 200 instrument operating in high-resolution mode at accelerating voltage 5 kV.

The surface chemistry of the films was investigated by Fourier transform infrared spectroscopy (FT-IR) measurements in the 4000–400 cm<sup>-1</sup> spectral range, which were carried out on TiO<sub>2</sub>-coated silicon substrates using a Bruker Equinox 70 FT-IR apparatus in transmission mode at a resolution of 4 cm<sup>-1</sup>. To compensate for possible changes in the positioning of the samples as well as in the thickness of the films, all the spectra were normalized to the TiO<sub>2</sub> absorption at 800 cm<sup>-1</sup>, which was previously verified to be insensitive to any UV or post-UV storage treatments.<sup>38,39</sup> A peak deconvolution procedure was applied to the spectra using the Levenberg–Marquardt method, as described previously.<sup>38</sup> The accuracy of the fit was estimated by the goodness-of-fit statistical indicator of the software.

The wettability of the TiO<sub>2</sub> films was evaluated by water contact angle (WCA) measurements performed by the sessile drop method using a CAM200-KSV instrument (equipped with a digital camera for taking magnified images of the microdroplets). The tests were typically conducted by dispensing the droplets of bidistilled water (3 μL) by means of a

microsyringe. For each sample, the contact angle value was obtained as an average of 5 measurements recorded on different neighbouring surface locations on the basis of shape analysis performed by a CAM200-KSV software.

#### Irradiation/storage experiments

To induce hydrophilicity, the TiO<sub>2</sub> coatings were irradiated with the third harmonic wavelength (355 nm) of a pulsed Nd:YAG laser, with a pulse duration of 3 ns, a repetition rate of 10 Hz, and fluence of 7 mJ cm<sup>-2</sup> (measured by a Tektronik oscilloscope coupled with an energy meter). The laser spot had a 0.5 cm diameter and was always positioned in the center of the substrate slides to allow for the reproducible identification of the illuminated area. The total duration of the UV irradiation experiments was 120 min, corresponding to 72 000 laser pulses, and hence, to an actual interaction time of UV photons with the TiO<sub>2</sub> samples of only 0.216 ms.<sup>38</sup>

After UV irradiation, the TiO<sub>2</sub> films were subjected to different sets of storage conditions/stimulation, as follows: (i) storage in the dark under ambient environment (with relative humidity of 30–40%); (ii) heating in the dark by contacting the underlying Si substrate with a hot plate kept at 50–150 °C; (iii) irradiation of the film surfaces with laser pulses at  $\lambda_{\text{ex}} = 532$  nm and  $\lambda_{\text{ex}} = 1064$  nm (with repetition rate = 10 Hz, total fluence = 15 mJ cm<sup>-2</sup>) using simultaneously the second and the first harmonics of a Nd-YAG laser; (iv) sample storage under vacuum at a pressure of  $3 \times 10^{-3}$  mbar achieved by a rotary pump. Conditions (ii)–(iv) were hold for 40 h, following which further storage was allowed under ambient dark.

### 3. Results

#### 3.1 Morphological characterization of the TiO<sub>2</sub> films

In this work, we have carefully examined the wetting behaviour of TiO<sub>2</sub> NR thin-films with UV-switchable hydrophilicity. In order to circumvent extra wettability effects induced by micron-size structuring<sup>40</sup> and, hence, to simplify rationalization of the detectable effects, we have considered TiO<sub>2</sub> coatings with nanometer-scale roughness realized on flat silicon substrates. To this aim, OLAC-capped anatase (tetragonal) TiO<sub>2</sub> NRs have been synthesized by a low-temperature base-catalyzed hydrolysis of titanium tetraisopropoxide in OLAC as both solvent and promoter of anisotropic growth.<sup>41</sup> The representative low-magnification TEM image in Fig. 1a demonstrates that the NRs actually consist of uniformly sized and shaped nanocrystals with a rod-like profile and average short-/long-axis dimensions of ~3 nm/~25 nm, respectively. Prior to their utilization in film fabrication, the as-prepared NRs have been provided with fresh OLAC capping by means of a ligand-exchange procedure carried out under inert atmosphere, which allows the inner –C=C– double to be preserved from possible oxidative damages.<sup>47–48</sup> TiO<sub>2</sub> coatings (typically ~300–500 nm in thickness) made of NRs arranged in laterally close-packed assemblies have been fabricated at room temperature by transferring NR films floating at a water/air interface to Si substrates by a sequential dipping/withdrawal procedure carried out at controlled rate. The representative SEM overview in Fig. 1b

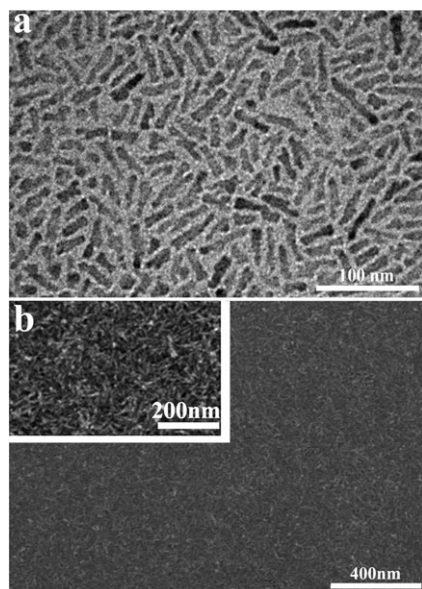


**Fig. 1** (a) Low-magnification TEM image of the as-synthesized TiO<sub>2</sub> nanorods (NRs). (b) SEM overview at different magnifications of a typical TiO<sub>2</sub> NR film on a silicon substrate.

shows that continuous, crack-free compact NR films are achieved on the substrates over areas as large as several squared micrometers without formation of micron-sized aggregates.

### 3.2 WCA characterization

In order to induce hydrophilicity, the TiO<sub>2</sub>-coated substrates have been excited with laser pulses at  $\lambda_{\text{ex}} = 355$  nm for 120 min, corresponding to a net photon-TiO<sub>2</sub> interaction time of 0.216 ms. The employed irradiation wavelength guarantees maximized absorption by the TiO<sub>2</sub> component, while the low repetition rate ensures negligible heat production within the films.<sup>38</sup> Fig. 2 summarizes the typical evolution of the WCA values for samples subjected to UV irradiation/storage cycles. The as-prepared TiO<sub>2</sub> NR coatings display a WCA of about  $\sim 100^\circ$  (Fig. 2b) that is considerably higher than the values reported in literature for both polycrystalline TiO<sub>2</sub> films and single-crystalline surfaces ( $50$ – $60^\circ$ ).<sup>3,15–34</sup> Such an elevated degree of hydrophobicity is ascribable to the synergistic contributions from the nonpolar character of the OLAC molecules capping individual NRs and from the nanometer-scale roughness of the film surface, which is naturally imparted by the attained organization of the NR building blocks in compact multilayers lying approximately parallel to the substrate underneath (*cf.* Fig. 1b).<sup>38,39</sup> Pulsed UV irradiation for 120 min is sufficient to convert the wettability of the substrates to a very hydrophilic state featured by a WCA close to less than  $\sim 20^\circ$  (Fig. 2b).<sup>38–40</sup> The post-UV wettability changes exhibited by the films have been then monitored by applying the following sets of storage conditions/stimulation for 40 h, while taking the corresponding recovery kinetics under ambient laboratory environment in the dark as a reference:

- sample storage under vacuum;
- heating by contacting the underlying Si substrate with a hot plate (as a representative case of study, we report on the

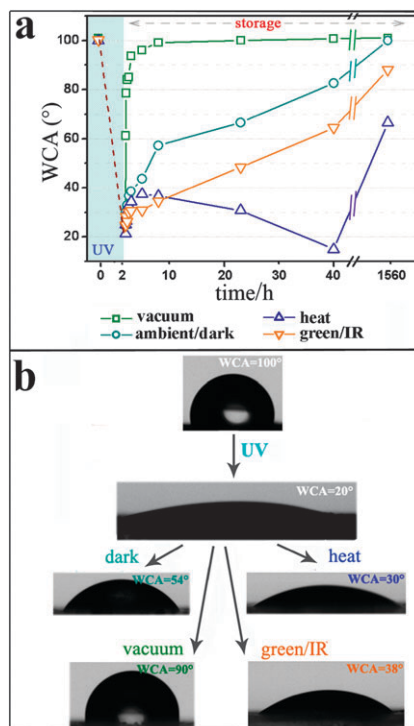


**Fig. 2** (a) Water contact angle (WCA) measurements performed on distinct TiO<sub>2</sub> NR film samples at scheduled time intervals following pulsed UV irradiation and prolonged storage under: (i) ambient laboratory atmosphere in the dark; (ii) vacuum; (iii) hot-plate heating; (iv) green/IR laser irradiation. Conditions (ii)–(iv) were kept for 40 h, following which further storage was allowed under ambient dark conditions. (b) Optical images of a water droplet in contact with TiO<sub>2</sub> NR films before UV irradiation, and after UV irradiation followed by 5 h storage under different conditions.

results of heating at  $100^\circ\text{C}$ , *i.e.*, close to the boiling point of water);

(c) irradiation of the film surfaces with laser pulses at  $\lambda_{\text{ex}} = 532$  nm and  $\lambda_{\text{ex}} = 1064$  nm (such double-wavelength illumination conditions was selected in order to mimic qualitatively the irradiation regime used in previously reported light-assisted recovery experiments).<sup>35</sup>

The comparative overview in Fig. 2a highlights that the wettability changes exhibited by the NR films after their UV-induced hydrophilicization depend strongly on the specific storage conditions applied. From the collected data, it clearly emerges that the WCA increases abruptly only upon vacuum application. For example, it can be appreciated that the coatings kept under vacuum exhibit an increase in the WCA up to about  $60^\circ$  in less than 1 h. In contrast, a similar wetting status is achieved after  $\sim 14$  h,  $\sim 35$  h, or  $\sim 1500$  h for films stored in the dark, or subjected to green/IR irradiation or heating, followed by dark storage, respectively. Vacuum storage ultimately allows complete recuperation of the pristine pre-UV hydrophobicity in about 5 h, after which no further changes can be noticed (Fig. 2b). As opposed, the dehydrophilicization process proceeds at a remarkably slower rate with all of the other alternative methods (Fig. 2a). In particular, while only a slight variation in the slope of the time-dependent wettability curves is identifiable at around 6–10 h both for the

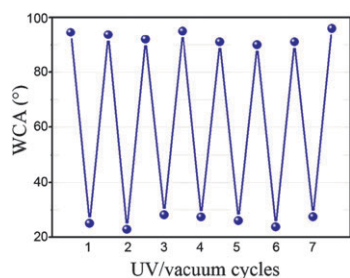


**Fig. 3** Reversible wettability changes of TiO<sub>2</sub> NR coatings during cyclic alternations of 120 min pulsed UV illumination and 5 h storage in vacuum the repeated UV-vacuum storage. No significant fatigue can be noted.

green/IR treated and the naturally stored samples, the use of heating leads to a more complex three-stage behaviour. Actually, the WCA slightly increases during the first 3–5 h, after which it steadily declines approaching a hydrophilic degree even slightly higher than that observed after UV irradiation (WCA  $\approx 15^\circ$  at  $\sim 40$  h). Subsequently, a renewed WCA increase is detected. As a matter of fact, it is observable that the full hydrophobicity recovery (*i.e.*, WCA  $\sim 100^\circ$ ) is reached after a period as long as 1560 h (65 days) exclusively under dark ambient conditions, whereas only partial recuperation is ultimately achieved by assisting the initial 40 h storage with green/IR or heat (WCA  $\approx 90^\circ$  C and  $\approx 65^\circ$ , in the respective cases).

For the specific type of colloidal TiO<sub>2</sub> films investigated here, it appears clear that application of post-UV vacuum is an extremely efficient strategy permitting fast and full recovery of the original wettability responses. In order to check the suitability of such systems for practical applications, the repeatability of the switchable WCA values TiO<sub>2</sub> has been examined. Fig. 3 demonstrates that the process of hydrophilicization/hydrophobicization within the  $\sim 100^\circ$ – $20^\circ$  WCA interval can be safely carried out over several cycles of alternating 120 min pulsed UV irradiation and vacuum storage periods as short as 5 h (*cf.* Fig. 2). The data prove that the NR coatings indeed exhibit excellent reversibility in their wettability properties without being detrimentally affected by any apparent fatigue, as similarly assessed for samples that are allowed to recuperate (although comparatively more slowly) under dark ambient conditions.<sup>38–40</sup> In contrast, corresponding repeatability assessment experiments, in which the post-UV recovery was assisted by either green/IR or hot plate heating showed progressive attenuation of the ultimate wettability excursions with increasing the number of cycles (data not shown), which actually suggests the occurrence of irreversible degradation phenomena under such storage modes.

### 3.3 FT-IR characterization

In order to elucidate the mechanism responsible for the diverse recovery dynamics, the temporal evolution of the main vibrational modes associated with the organic components TiO<sub>2</sub> NR films have been monitored by means of FT-IR spectroscopy over 40 h of post-UV storage. At the end of such periods (*cf.* Fig. 2), the vacuum-treated films have reverted back to the initial WCA  $\approx 100^\circ$  since long, the sample stored under

ambient conditions and subjected to green/IR stimulation have attained only partial WCA restoration to  $\approx 83^\circ$  and  $65^\circ$ , respectively, whereas the heated samples have instead become more hydrophilic with WCA  $\approx 15^\circ$ . The results are summarized in Fig. 4, in which the evolution of the full FT-IR spectra is reported, and in Fig. 5, in which the relative time-dependent changes of the most informative sets of stretching ( $\nu$ ) and bending ( $\delta$ ) vibrations, obtained by peak deconvolution analysis, are shown (note that, in order to allow for a comparative evaluation, the peak areas relative to the O–H vibrations in Fig. 4a–b were normalized to their respective values recorded *immediately after* UV irradiation, while the peak areas relative to the C–H vibrations in Fig. 4c were normalized to their respective initial values *prior to* UV irradiation).

In the 3600–1000  $\text{cm}^{-1}$  interval, the as-prepared (*i.e.* unirradiated) TiO<sub>2</sub> NR films (black traces in all of the panels of Fig. 4) show the characteristic bands of OLAC molecules bound to the surface of the NRs,<sup>38</sup> including the olefinic and methyl/methylene groups in the alkyl chain (with  $\nu(\text{C}=\text{H})$  at  $\sim 3005 \text{ cm}^{-1}$  and  $\nu(\text{CH}_3/\text{CH}_2)$  between 2900–2800  $\text{cm}^{-1}$ , respectively), carboxylate anions of OLAC coordinated to surface Ti atoms in chelating bidentate binding mode (a double band peaking at  $\nu(-\text{CO}_2^-) \approx 1520$  and  $\approx 1430 \text{ cm}^{-1}$ , respectively), carbonyl moieties of protonated carboxylic heads of OLAC, which form unidentate surface complexes *via* their alkyl oxygen atom ( $\nu(\text{C}=\text{O}) \approx 1710 \text{ cm}^{-1}$ ). The broad and weak stretching band of hydroxyl groups at  $\nu(\text{O}=\text{H})=3600\text{--}2800 \text{ cm}^{-1}$  suggests that a few titanol groups, TiO–H (commonly referred to as dissociatively adsorbed H<sub>2</sub>O) and/or molecularly physisorbed H<sub>2</sub>O already contaminate the NR surface.<sup>41</sup> The broad featureless  $\nu(\text{Ti}=\text{O})$  signature of the TiO<sub>2</sub> lattice vibrations can be clearly observed below  $\sim 1000 \text{ cm}^{-1}$ . Taken together, these FT-IR analyses are fully consistent with the fact that the colloidal NRs composing the films are individually enwrapped within a surface shell of OLAC molecules that are directly anchored to the exposed TiO<sub>2</sub> facets *via* their carboxylic heads while exposing the alkyl chains outwards. Such surfactant surface protection on the NR building blocks attributes a pronounced hydrophobic character to films, as authenticated by a WCA value of the order of  $\sim 100^\circ$  (Fig. 2).<sup>38</sup>

Following pulsed UV-treatment the films attain a generally higher degree of the TiO<sub>2</sub> surface hydroxylation that is corroborated by a considerable increase in the  $\nu(\text{O}=\text{H})$  vibrations due to the convoluted contributions from growing TiO–H species and physisorbed H<sub>2</sub>O at  $\sim 3400 \text{ cm}^{-1}$  and  $\sim 3200 \text{ cm}^{-1}$ , respectively (*cf.* light blue traces in Fig. 4 and Fig. 5a–b). The latter attributions are in agreement with the strong enhancement of the  $\delta(\text{O}=\text{H})$  vibration at  $\sim 1640 \text{ cm}^{-1}$  which is indeed a signature of the presence of molecularly adsorbed (*i.e.*, undissociated) H<sub>2</sub>O (Fig. 4). Concomitantly, the UV irradiation causes a moderate attenuation for the  $\nu(\text{C}=\text{H})$  and  $\nu(\text{CO}_2^-)$  bands of the OLAC ligands (*cf.* Fig. 4 and Fig. 5c). As a coherent macroscopic result of a renovated surface environment embodying a rich density of O–H species and OLAC ligands, the UV-irradiated TiO<sub>2</sub> films exhibit a highly hydrophilic state featured by WCA as low as  $20^\circ$  (Fig. 2).



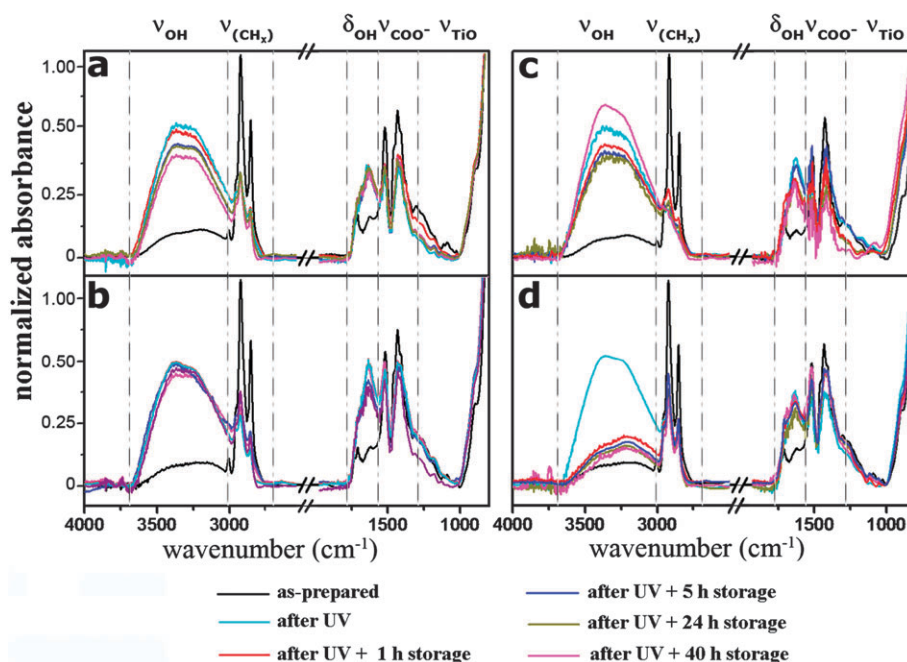


**Fig. 4** FT-IR time evolution of the surface chemistry of distinct TiO<sub>2</sub> NR films after 120 min pulsed UV irradiation and varying storage periods under different conditions: (a) under ambient laboratory atmosphere in the dark; (b) under pulsed green/IR laser irradiation; (c) on a hot plate heated up to 100 °C; (d) under vacuum produced by a rotary pump. To compensate for possible changes in the positioning of the samples as well as in the thickness of the films, all the spectra were normalized to the TiO<sub>2</sub> absorption at 800 cm<sup>-1</sup>.

Comparative examination of the time-dependent data in Fig. 4 and Fig. 5 reveals that the investigated storage conditions impact on the evolution of the film chemistry to a strongly variable extent. As for what concerns the spectral evolution associated with the samples subjected to either ambient storage and vacuum treatment, it is noted that the most prominent alterations in  $\nu(\text{O-H})$  and  $\delta(\text{O-H})$  bands (of the order of 80% and 20%, respectively) occur over the first 10 h of storage, along with moderate enhancement in C-H vibrations of the OLAC ligands (by 25% and 5%, respectively), after which further evolution occurs steadily, although at reduced rate. The minor non-monotonic changes in the  $\nu(\text{CO}_2^-)$  features could be presumably ascribed to rearrangements of the binding configuration of carboxylic heads on the TiO<sub>2</sub> surfaces.<sup>38</sup>

By comparison, the application of green/IR irradiation to the hydrophilized is accompanied by a slower  $\nu(\text{O-H})/\delta(\text{O-H})$  removal process and almost negligible  $\nu(\text{C-H})$  recuperation (Fig. 5).

In the case of the heat-assisted recovery, the vibrational bands do not follow any monotonic behaviour. Actually, the  $\nu(\text{O-H})/\delta(\text{O-H})$  intensities decrease during the first 20 h by about 40%, reaching a minimum, after which they even recuperate to value obtained immediately after UV irradiation (Fig. 5a–b). Concomitantly, minor  $\nu(\text{C-H})$  recuperation (by less than 5%) takes place over the first 20 h, after which the related signals are permanently depressed well below the intensity level attained immediately after the UV irradiation (Fig. 5c).

Finally, it deserves emphasizing that control experiments carried out on unirradiated NR films have not evidenced any significant variations in their WCA and/or in the associate

vibrational features after being subjected to either of the concerned storage conditions. In addition UV-hydrophilicization/storage experiments conducted on organic-free TiO<sub>2</sub> NR films (from which the OLAC coating has been photocatalytically removed under continuous illumination with a conventional cw 500 W Xe lamp<sup>38</sup>) have not been accompanied by emergence of any detectable  $\nu(\text{C-H})/\nu(\text{CO}_2^-)$  signals over time. These facts discredit the hypothesis that the inherent wettability and/or the surface features of the as-prepared NR films could be modified upon adsorption/desorption of atmospheric hydrocarbon and/or water.

#### 4. Discussion

Upon pulsed UV irradiation, the TiO<sub>2</sub> NR coatings can convert from a highly hydrophobic to a highly hydrophilic state, a transition that is accompanied by an increased degree of TiO<sub>2</sub> surface hydroxylation. On the other side, except for the heat-treated samples, the recovery behaviour of the film hydrophobicity, as marked by corresponding variations in the WCA values (*cf.* Fig. 2 and Fig. 4,5), generally correlates well with a gradual abatement of the O-H signals (which indicates progressive dehydroxylation), concomitant to slow recuperation of the C-H bands.

In particular, it emerges that the spectral evolution associated with the samples subjected to either ambient storage and vacuum treatment closely adheres to an inverted behaviour as compared to that observed during the forward UV-driven hydrophilicization. The latter observations allow us to deduce that the UV-driven wetting properties of the TiO<sub>2</sub> films that are reversed either naturally or under vacuum storage should be directly traced back to the flexible, concerted



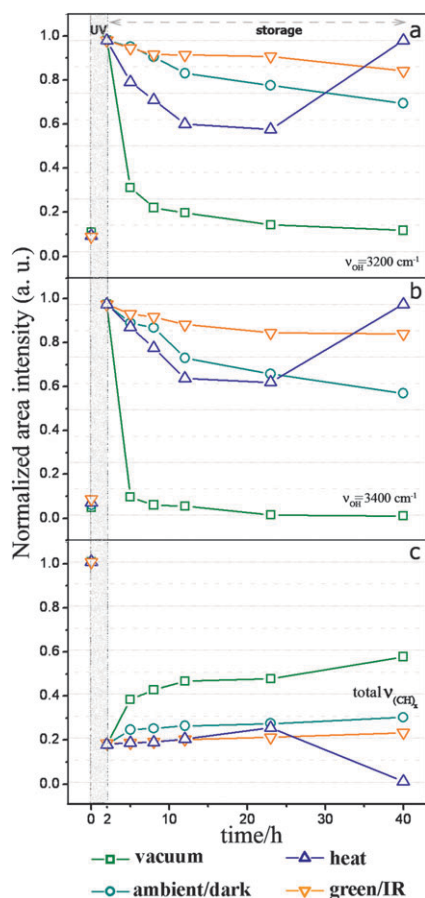


**Fig. 5** Temporal evolution of the peak area for relevant vibrations: O–H stretching at  $3200\text{ cm}^{-1}$  (a) and  $3400\text{ cm}^{-1}$  (b), respectively; total C–H stretching bands at  $2960\text{ cm}^{-1}$ ,  $2920\text{ cm}^{-1}$  and  $2860\text{ cm}^{-1}$  (c), respectively, determined by Levenberg–Marquadt deconvolution analysis of FT-IR spectra recorded at scheduled time intervals (as shown in Fig. 4). The peak areas relative to the O–H vibrations in panels (a)–(b) were normalized to their respective values recorded immediately after UV irradiation, while the peak area values relative to the C–H vibrations in panel (c) were normalized to their respective initial values prior to UV irradiation.

changes in the polar and nonpolar components of the  $\text{TiO}_2$  surface chemistry, as pointed out earlier.<sup>38</sup> On the other side, the finding that the original hydrophobicity of the samples can be ultimately recovered upon removal of O–H species despite the intensity of the C–H bands is not fully recuperated, supports our previously proposed mechanistic picture, according to which the surfactants could indeed respond to the hydroxylation/dehydroxylation processes by rearranging conformationally without being necessarily degraded.<sup>38</sup>

Similar arguments can be invoked to interpret the effects of green/IR light in assisting the post-UV recovery period. Under these circumstances, the slower  $\nu(\text{O–H})/\delta(\text{O–H})$  removal process and almost negligible  $\nu(\text{C–H})$  recuperation can be correlated with the observable decelerated dehydrophilicization and the incomplete recovery of the pre-UV hydrophobicity degree (Fig. 2). This finding therefore suggests that the extended lifetime of the hydrophilic state upon green/IR irradiation results from the  $\text{TiO}_2$  surfaces retaining

a moderately high polar character while also undergoing partial deactivation/elimination of the nonpolar components.

Differently, the impact of heating appears to be less straightforward to rationalize, as the associate vibrational band changes follow a non-monotonic three-phase behaviour. Among the various observations reported, the fact that the  $\nu(\text{C–H})$  signal intensity is decreased well below the post-UV value in spite of minor recuperation in the first 20 h of storage (Fig. 5c), clearly points to irreversible loss of nonpolar surface species. Such loss can account for the trend toward enhanced hydrophilicity which culminates at 40 h storage with WCA  $< 15^\circ$  that is even lower than the value induced by UV treatment itself. Additionally, it is noted that the sole convolution of the time-dependent changes of the polar and nonpolar components of the surfaces does not satisfactorily fit to three-phase changing behaviour of the WCA. Major discrepancies can be identified at the latest storage stages ( $>> 40$  h), at which renovated dominance of the O–H species coincides with hydrophobicity recuperation up to WCA  $\approx 60^\circ$ . Such unusual behaviour is likely to originate from structural heat-induced modifications in the  $\text{TiO}_2$  films taking place along OLAC removal, such as reorganization of the NR packing mode and/or introduction of different surface geometries, which could complicate the ultimate wetting behaviour due to transition through diverse wetting regimes.<sup>1,2,40</sup>

The detailed pathways the hydrophilicization/dehydrophilicization processes underlying the investigated wettability changes deserve further discussion. Our experiments are mostly consistent with previous mechanistic explanations.<sup>3,15–17,19–21</sup> Band-gap  $\text{TiO}_2$  photoexcitation would induce formation of oxygen vacancies on  $\text{TiO}_2$  surfaces, at which ambient  $\text{H}_2\text{O}$  could compete kinetically with  $\text{O}_2$  for adsorption, eventually dissociating into Ti–H groups. As ligand coverage on colloidal nanocrystals is usually incomplete, the NRs can be expected to carry surfactant-free surface regions of nanometer-scale extension. Such domains are believed to serve as a primary ground for molecular and/or dissociative adsorption of atmospheric  $\text{H}_2\text{O}$ , thereby initiating  $\text{TiO}_2$  hydrophilicization.<sup>38</sup> An increasing density of such newly introduced O–H species could, in turn, promote adhesion of  $\text{H}_2\text{O}$  multilayers, leading to the formation of highly hydrophilic surface regions on the NR facets. Overall, UV irradiation would produce an alternating distribution of nanoscale surface region with either hydrophilic (related to the newly implanted O–H moieties) or hydrophobic character (associated with surfactant-passivated areas of the NRs) throughout the porous NR films, which could give rise to a two- and three-dimensional nanocapillary infiltration effect, allowing water droplets to spread out over the  $\text{TiO}_2$  coatings.<sup>15,16,38</sup>

As a matter of fact, OH-healed  $\text{TiO}_2$  surfaces are known to be metastable. Therefore, it can be easily understood that, with the lack of oxygen vacancies being continuously regenerated exclusively under UV illumination,  $\text{O}_2$  substitution for the previously implanted O–H moieties, which is indeed thermodynamically favoured, can dominate over  $\text{H}_2\text{O}$  adsorption during prolonged periods of air storage in the dark. Back-reconstruction proceeds at a comparatively faster rate in the initial period of dark storage, after which further relaxation is slowed down, indicating that the recovery kinetics depends on

the actual density of O–H moieties. Overall, establishment of the new near-equilibrium conditions at the TiO<sub>2</sub> surface is an extremely slow process, which could be in fact facilitated only supplying extra doses of O<sub>2</sub> under an artificially adjusted atmosphere.<sup>21</sup>

On the other hand, the temporary nature that characterizes the intensity alterations in the OLAC bands under natural storage conditions cannot be explained by the occurrence of irreversible photocatalytic degradation and/or abstraction of the capping OLAC shell, but most likely arises from the bound surfactants undergoing conformational changes in response to surface hydroxylation/dehydroxylation events.<sup>38–40</sup> Actually, substantial geometric rearrangements can be expected to lead to alterations in the characteristic intensity and frequency of their vibrational modes.<sup>42–44</sup> Changes in NR-to-NR hydrophobic interactions could, in turn, affect the back-conformational rearrangements in the dark, so that the vibrational behaviour that accompanies the forward and reverse processes may differ to some extent. Regardless of this, such a mechanism implies preservation of the nonpolar surface micro-environment associated with the alkyl chains of OLAC ligands.

The inherent metastability of the OH-healed TiO<sub>2</sub> surfaces is further manifested by the effect of applying vacuum to the hydrophilicized films. In the lack of oxygen at such reduced pressures, the most plausible mechanism that could be operative should involve continuous subtraction of surface bound O–H species from TiO–H, molecularly physisorbed H<sub>2</sub>O, and H-bonded H<sub>2</sub>O multilayers, in the form of gaseous H<sub>2</sub>O and possibly H<sub>2</sub>O<sub>2</sub> molecules.<sup>45,46</sup> However, vacuum-driven O–H removal may not necessarily result in formation of surface oxygen vacancies similar to those primarily induced by the forward UV photocorrosion. In fact, under such circumstances highly reactive surfaces would be produced, which could be expected to be susceptible to be suddenly hydroxylated again once put in contact with the ambient pressure atmosphere. However, the attained increase in WCA remains stable, therefore indicating that any hydroxylation is disfavoured on such vacuum-reconstructed surfaces.

For durable and reversibly switchable wettability to be achieved between hydrophobic/hydrophilic extremes, dynamic changes in the degree of TiO<sub>2</sub> hydroxylation, on one side, and preservation of the alkyl chains of the OLAC ligands, on the other side, should be ensured throughout a number of alternating UV/storage cycles. It has been previously established that the selective, pulsed UV irradiation conditions employed in our experiments meet both requirements in the forward UV-driven hydrophilicization stage.<sup>38</sup> The present experimental data demonstrate that vacuum application allows the pre-UV hydrophobicity state to be recovered by reverting back the UV-altered polar and nonpolar components of the TiO<sub>2</sub> surface chemistry to their original conditions. Although a similar reversible wettability can be observed upon storage under natural ambient conditions, however the overall vacuum-driven dehydrophilicization demonstrates to be a ~250-times faster process.

The slower and incomplete wettability recovery under either green/IR illumination or heating should be related to the induced stimulation of vibrational modes of both the TiO<sub>2</sub> lattice and of OLAC surfactants. This could lead to two main

effects. First, OLAC ligands may be driven to take configurations hindering the OH/H<sub>2</sub>O desorption from the TiO<sub>2</sub> surface, thus imposing a hydrophilic character for a longer time. Second, some photodegradation pathways can come into play, for example, upon photodesorption and/or rupture of chemical bonds, followed by reaction of the resulting radicals with atmospheric oxygen.<sup>47,48</sup> Consequent depletion of O<sub>2</sub> availability in proximity of the TiO<sub>2</sub> surfaces would further contribute to slow down the dehydroxylation of the OH-healed surfaces. The slow decay of the  $\nu(\text{OH})$  vibrations under green/IR light, on one side, and their unexpected huge increase after prolonged heating on the other side, can be partly be rationalized on the basis of OLAC degradation into hydroxylated by-products with low molecular weight.<sup>49,50</sup> As highlighted by our data, the impact of direct hot-plate heating appears to be considerably pronounced, likely due to the broader spectrum of excitable vibrations, as compared to what can be achieved by the wavelength-selective green/IR stimulation. Actually, the susceptibility of the OLAC capping to be photo-oxidized is dramatically accentuated under the former circumstances.

## 5. Conclusions

We have examined the wettability evolution of compact TiO<sub>2</sub> thin films made of surfactant-capped nanocrystals, which can convert from a highly hydrophobic state to a highly hydrophilic and metastable one under UV irradiation. Combined FT-IR and WCA investigations have provided detailed mechanistic information on the impact of post-UV storage on the properties of such types of films. It has been understood that achieving switchability between extreme wettability excursions as well as long-term repeatability of such changes requires dynamic modifications in the polar and nonpolar components of the TiO<sub>2</sub> films, which are related to newly introduced OH moieties, on one side, and to alkyl chains of the capping molecules, on the other side. The relevant roles played by such pre-existing organic components explain why the responses of the as-hydrophilicized films to either visible/IR or heat stimulation diverge significantly from those reported for conventional organic-free polycrystalline TiO<sub>2</sub> surfaces.<sup>21,32–35</sup> The application of moderate vacuum is found to be an effective tool to accelerate the post-UV hydrophilic-to-hydrophobic conversion, thereby enabling cyclic hydrophilicization/hydrophobicization alternation without any detrimental fatigue.

Overall, the present study further highlights that largely varying mechanisms can concur to determine the ultimate TiO<sub>2</sub> wetting switchability, the relative extent of which can be expected to depend on the specific features of the concerned surfaces and on the particular irradiation/storage conditions applied. Our findings may be useful to suggest additional criteria to engineer light-responsive, TiO<sub>2</sub>-based organic-inorganic functional surfaces with controllable wettability properties for tailored applications, *e.g.* in microfluidics.

## Acknowledgements

Financial support from the Italian Ministry of Research (contract no. RBIN048TSE) is acknowledged. The authors thank Benedetta Antonazzo for performing SEM measurements.

## References

- 1 T. Sun, L. Feng, X. Gao and L. Jiang, *Acc. Chem. Res.*, 2005, **38**, 644.
- 2 X. J. Feng and L. Jiang, *Adv. Mater.*, 2006, **18**, 3063.
- 3 T. L. Thompson and J. T. Yates, *Chem. Rev.*, 2006, **106**, 4428.
- 4 X. M. Li, D. Reinhoudt and M. Crego-Calama, *Chem. Soc. Rev.*, 2007, **36**, 1350.
- 5 A. Fujishima and X. Zhang, *C. R. Acad. Sci., Ser. IIC: Chim.*, 2006, **9**, 750.
- 6 S. Wang, Y. Song and L. Jiang, *J. Photochem. Photobiol., C*, 2007, **8**, 18.
- 7 L. Xu, W. Chen, A. Mulchandani and Y. Yan, *Angew. Chem., Int. Ed.*, 2005, **44**, 6009.
- 8 X. Yu, Z. Wang, Y. Jiang, F. Shi and X. Zhang, *Adv. Mater.*, 2005, **17**, 1289.
- 9 A. Athanassiou, M. I. Lygeraki, D. Pisignano, K. Lakiotaki, M. Varda, E. Mele, C. Fotakis, R. Cingolani and S. H. Anastasiadis, *Langmuir*, 2006, **22**, 2329.
- 10 F. Di Benedetto, E. Mele, A. Camposeo, A. Athanassiou, R. Cingolani and D. Pisignano, *Adv. Mater.*, 2008, **20**, 314.
- 11 S. Wang, H. Liu, D. Liu, X. Ma, X. Fang and L. Jiang, *Angew. Chem., Int. Ed.*, 2007, **46**, 3915.
- 12 X. Feng, L. Feng, M. Jin, J. Zhai, L. Jiang and D. Zhu, *J. Am. Chem. Soc.*, 2004, **126**, 62.
- 13 S. Wang, X. Feng, J. Yao and L. Jiang, *Angew. Chem., Int. Ed.*, 2006, **45**, 1264.
- 14 H. S. Lim, D. Kwak, D. Y. Lee, S. G. Lee and K. Cho, *J. Am. Chem. Soc.*, 2007, **129**, 4128.
- 15 R. Wang, K. Hashimoto, A. Fujishima, M. Chikuni, E. Kojima, A. Kitamura, M. Shimohigoshi and T. Watanabe, *Nature*, 1997, **388**, 431.
- 16 R. Wang, K. Hashimoto, A. Fujishima, M. Chikuni, E. Kojima, A. Kitamura, M. Shimohigoshi and T. Watanabe, *Adv. Mater.*, 1998, **10**, 135.
- 17 X. J. Feng, J. Zhai and L. Jiang, *Angew. Chem., Int. Ed.*, 2005, **44**, 5115.
- 18 X. Zhang, M. Jin, Z. Liu, D. A. Tryk, S. Nishimoto, T. Murakami and A. Fujishima, *J. Phys. Chem. C*, 2007, **111**, 14521.
- 19 N. Sakai, A. Fujishima, T. Watanabe and K. Hashimoto, *J. Phys. Chem. B*, 2003, **107**, 1028.
- 20 F. K. Lee, G. Andreatta and J. J. Benattar, *Appl. Phys. Lett.*, 2007, **90**, 181928.
- 21 R. Wang, N. Sakai, A. Fujishima, T. Watanabe and K. Hashimoto, *J. Phys. Chem. B*, 1999, **103**, 2188.
- 22 C. Y. Wang, H. Groenzin and M. J. Shultz, *Langmuir*, 2003, **19**, 7330.
- 23 J. M. White, J. Szanyi and M. A. Henderson, *J. Phys. Chem. B*, 2003, **107**, 9029.
- 24 T. Zubkov, D. Stahl, T. L. Thompson, D. Panayotov, O. Diwald and J. T. Yates, *J. Phys. Chem. B*, 2005, **109**, 15454.
- 25 M. Takeuchi, K. Sakamoto, G. Martra, S. Coluccia and M. Anpo, *J. Phys. Chem. B*, 2005, **109**, 15422.
- 26 M. Takeuchi, G. Martra, S. Coluccia and M. Anpo, *J. Phys. Chem. C*, 2007, **111**, 9811.
- 27 X. Zhang, M. Jin, Z. Liu, S. Nishimoto, H. Saito, T. Murakami and A. Fujishima, *Langmuir*, 2006, **22**, 9477.
- 28 N. Sakai, A. Fujishima, T. Watanabe and K. Hashimoto, *J. Phys. Chem. B*, 2001, **105**, 3023.
- 29 M. Miyauchi, *J. Mater. Chem.*, 2008, **18**, 1858.
- 30 M. Miyauchi, A. Nakajima, T. Watanabe and K. Hashimoto, *Chem. Mater.*, 2002, **14**, 4714.
- 31 M. Miyauchi, A. Nakajima, K. Hashimoto and T. Watanabe, *Adv. Mater.*, 2000, **12**, 1923.
- 32 K. Katsumata, A. Nakajima, T. Shiota, N. Yoshida, T. Watanabe, Y. Kameshima and K. Okada, *J. Photochem. Photobiol., A*, 2006, **180**, 75.
- 33 N. Sakai, R. Wang, A. Fujishima, T. Watanabe and K. Hashimoto, *Langmuir*, 1998, **14**, 5918.
- 34 A. Nakajima, S. I. Koizumi, T. Watanabe and K. Hashimoto, *J. Photochem. Photobiol., A*, 2001, **146**, 129.
- 35 M. Miyauchi, N. Kieda, S. Hishita, T. Mitsuhashi, A. Nakajima, T. Watanabe and K. Hashimoto, *Surf. Sci.*, 2002, **511**, 401.
- 36 D. S. Kommireddy, A. A. Patel, T. G. Shutava, D. K. Mills and Y. M. Lvov, *Small*, 2005, **5**, 1081.
- 37 D. Lee, M. F. Rubner and R. E. Cohen, *Nano Lett.*, 2006, **6**, 2305.
- 38 G. Caputo, C. Nobile, T. Kipp, L. Blasi, V. Grillo, E. Carlino, L. Manna, R. Cingolani, P. D. Cozzoli and A. Athanassiou, *J. Phys. Chem. C*, 2008, **112**, 701.
- 39 G. Caputo, C. Nobile, R. Buonsanti, T. Kipp, L. Manna, R. Cingolani, P. D. Cozzoli and A. Athanassiou, *J. Mater. Sci.*, 2008, **43**, 3474.
- 40 G. Caputo, B. Cortese, C. Nobile, M. Salerno, R. Cingolani, G. Gigli, P. D. Cozzoli and A. Athanassiou, *Adv. Funct. Mater.*, 2009, DOI: 10.1002/adfm.200800909.
- 41 P. D. Cozzoli, A. Kornowski and H. Weller, *J. Am. Chem. Soc.*, 2003, **125**, 14539.
- 42 N. C. Chia and R. Mendelsohn, *J. Phys. Chem.*, 1992, **96**, 10543.
- 43 W. Gao, L. Dickinson, C. Grozinger, F. G. Morin and L. Reven, *Langmuir*, 1996, **12**, 6429.
- 44 G. Srinivasan, M. Pursch, L. C. Sander and K. Muller, *Langmuir*, 2004, **20**, 1746.
- 45 O. Bikondoa, C. L. Pang, R. Ithnin, C. A. Muryn, H. Onishi and G. Thornton, *Nat. Mater.*, 2006, **5**, 189.
- 46 Y. Du, N. A. Deskins, Z. Zhang, Z. Dohnalek, M. Dupuis and I. Lyubinetzky, *J. Phys. Chem. C*, 2009, **113**, 666.
- 47 S. S. Lin, A. L. Hsieh, D. B. S. Min and S. S. Chang, *J. Am. Oil Chem. Soc.*, 1976, **53**, 157.
- 48 A. Nakajima and H. Hidaka, *J. Photochem. Photobiol., A*, 2003, **74**, 189.
- 49 T. Minabe, D. A. Tryk, P. Sawunyama, Y. Kikuchi, K. Hashimoto and A. Fujishima, *J. Photochem. Photobiol., A*, 2000, **137**, 53.
- 50 M. Tedetti, K. Kawamura, M. Narukawa, F. Joux, B. Charrière and R. Sempéré, *J. Photochem. Photobiol., A*, 2007, **188**, 135.